

Charge trapping on defects in AlGa_N/Ga_N field effect transistors

Oleg Mitrofanov* and M.J. Manfra

Bell Laboratories, Alcatel-Lucent, 600 Mountain Ave, Murray Hill, NJ 07974, USA

Keywords: trap, defect, GaN, transistor.

ABSTRACT

The presence of electronic traps in GaN-based devices limits device performance and reliability. Crystallographic defects in the bulk and electronic states on the surface act as trapping centers. We review the trapping phenomena in GaN-based high electron mobility transistors and discuss a characterization method, current transient spectroscopy, applied for trap identification. Probing the charge trapping mechanisms allows us to extract the trap characteristics including the trapping potential, the binding energy of an electron on the trap, and the physical location of the active centers in the device.

INTRODUCTION

GaN-based electronic devices have recently demonstrated excellent performance at microwave frequencies and tremendous potential in a variety of applications. However, quality of GaN material is still lacking that of mature technologies. Presence of dislocations and defects in large densities is one of the factors. In devices, defects act as charge trapping centers that limit the device performance. In AlGa_N/Ga_N high electron mobility transistors (HEMTs), the parasitic charge moving in and out of the traps on the surface and/or in the bulk of the heterostructure affects the density of the two dimensional electron gas (2DEG) in the channel, causing effects such as current collapse, and transconductance frequency dispersion.

Understanding the origin of the traps in GaN-based transistors, their location, and the physical mechanisms involved in the trapping is essential in device development. While the majority of the trapping effects result in similar degradation of the transistor characteristics at high frequencies, the dominating trapping mechanisms could vary in devices grown by different methods or subjected to different processing procedures. Transient spectroscopy allows extraction of the fundamental characteristics of the traps: the activation energy and the trap cross-section. A trapping center can be identified in different devices through these parameters. Extraction of the trap characteristics from the experimental data requires a theoretical understanding of the trapping process. Characteristics of the capture and emission process depend typically on the local temperature and the electric field. As a result, the apparent activation energy often significantly differs from the binding energy of the trap.

We discuss in detail one of the most commonly encountered manifestation of trapping in AlGa_N/Ga_N transistors: gate lag. We will focus on the physical properties of the traps, the mechanisms of the charge transfer, and the spatial location of the active traps in GaN transistors.

EXPERIMENT

In our experiments, the trapping dynamics is studied in Ga_N/AlGa_N/Ga_N HEMTs grown by plasma-assisted molecular beam epitaxy on semi-insulating SiC substrates. The heterostructure consists of $\sim 2 \mu\text{m}$ thick Ga_N buffer layer, a 30 nm Al_{0.34}Ga_{0.66}N barrier, and a 5 nm Ga_N capping layer. Strong piezoelectric and spontaneous polarization effects result in a formation of the two-dimensional electron gas (2DEG) at the AlGa_N/Ga_N interface. The density of the 2DEG is $\sim 1.2 \cdot 10^{13} \text{ cm}^{-2}$ and the room temperature mobility is $\sim 1400 \text{ cm}^2/\text{V s}$. The transistors are fabricated from the epilayers using optical contact lithography. A $1 \mu\text{m}$ long Schottky gate is deposited in the middle of the $5 \mu\text{m}$ long source-drain opening.

The dynamics of the electrons moving in and out of the traps is probed by measuring the induced charge in the transistor channel [1]. First, electrons are injected into the traps by applying a short negative filling pulse to the gate. The barrier height of the Schottky gate contact is sufficiently large (~ 1.0 - 1.5 eV), such that the probability of electron transfer by thermal activation is small. However, during the filling pulse, there is a large field across the AlGaIn barrier, which allows electrons to tunnel from the gate into the semiconductor. The number of the trapped electrons increases rapidly with the duration of the filling pulse and then saturates after ~ 10 μs [1]. In these experiments, however, filling pulses with duration of 1 μs and shorter are used to obtain trapped charge densities lower than the saturation level and to avoid emission enhancement due to Coulomb repulsion. As the gate potential returns to the initial value, the flow of electrons from the gate reduces and the concentration of the trapped electrons slowly returns to the equilibrium through emission processes.

The emission dynamics is directly reflected in the channel current transients. The field of the trapped electrons induces partial depletion of the 2DEG. The electron density variation is proportional to the amount of the trapped charge [1]. If a potential difference is applied between the source and the drain, a channel current transient that follows the filling gate pulse reflects the process of electron emission from the traps. The rate of current approach to the steady state level corresponds to the rate of electron emission from the traps.

In the experiment, the device is constantly biased in the common source configuration. Initially, the transistor is open and a steady state current I_D^{SS} is flowing in the channel. A filling pulse is applied to the gate every 50 ms. The drain current transient following the filling pulse is measured by a low insertion impedance 100 MHz bandwidth current probe. The electric field in the barrier of the HEMT consists of two components: the internal spontaneous polarization and the piezoelectric field of the heterostructure and the external electric field due to the potential difference between the gate contact and the transistor channel. At the potential difference of few volts, the external electric field magnitude exceeds values of 10^6 V/cm and becomes the major contribution to the total electric field in the barrier. For traps located in the barrier, dependence of the emission rate on the electric field is obtained by varying the drain potential. In the linear current regime (V_D is smaller than the knee voltage), the field in the barrier is directly proportional to the potential difference between the gate and the drain.

RESULTS

Typical normalized current transients $\Delta I(t) = I_D^{SS} - I_D(t)$ at different drain bias conditions at room temperature are shown in Fig. 1(a). To fill the traps, a 350 ns long filling pulse $V_G(t) = -3$ V is applied to the gate. The emission of the trapped charge that immediately follows the filling pulse is measured at $V_G = 0$ V. All the transients obtained at different

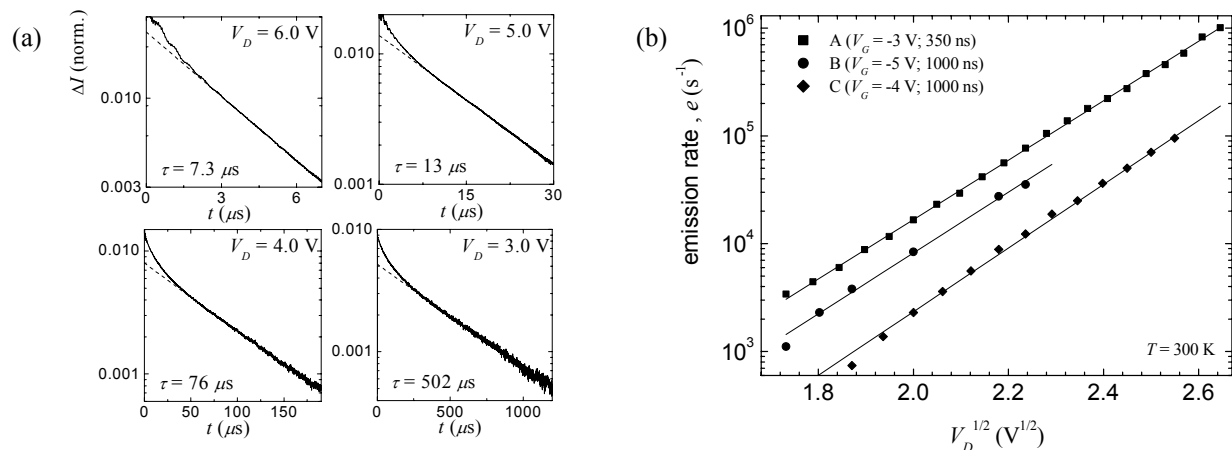


Fig. 1. Normalized current transients measured at different drain voltages (a) and the emission rate as a function of the square root of the applied voltage (b).

bias conditions show exponential approach to the steady state current level. The beginning of the transients contains a short non-exponential region, which we attribute to the emission enhancement due to the Coulomb repulsion. To obtain the emission rate, the long tail of the transient is fitted with the exponential decay function shown by the dash line.

The characteristic emission time $\tau = (e)^{-1}$ quickly decreases with the field strength F , suggesting that the emission from the trap is strongly assisted by the applied electric field. The functional dependence of the emission rate on the field can be determined by fitting the data $e(F)$ with a power law function ($\ln e = a + bV^p$). The result of the fitting indicates that the emission rate increases exponentially with the square root of the applied field. Figure 1(b) shows the emission rate as a function of the square root of the field measured on different wafers. The solid lines in the plot show fits to the data: $e = e(0)\exp(\alpha\sqrt{V_D})$. The physical meaning of $e(0)$ is the zero-field emission rate, and α is a constant that relates the applied voltage and the lowering of the trap potential. The zero-field emission rate varies from $0.003 \pm 0.001 \text{ s}^{-1}$ to $0.04 \pm 0.03 \text{ s}^{-1}$ for different wafers. On-wafer variation of the emission rate (for different devices) is insignificant. The values of constant α for different devices and wafers reside very closely to each other within the error bar $\alpha = 6.6 \pm 0.5 \text{ V}^{-1/2}$ ($T = 300 \text{ K}$).

The emission rate increases at elevated temperatures, suggesting the thermal nature of the emission process. The activation energy can be found from the slope of the logarithmic plot of eT^2 versus the inverse temperature. Figure 2 shows the emission rate measured at the bias conditions ranging from $V_D = 4.25 \text{ V}$ to $V_D = 5.75 \text{ V}$. The duration and the depth of the filling pulse are 1000 ns and -4 V respectively. In the temperature range of 250 K to 360 K the emission rate follows the Arrhenius behavior. The extracted activation energy is shown in the inset; it decreases with the applied field from $0.14 \pm 0.005 \text{ eV}$ at $V_D = 4.25 \text{ V}$ to $0.089 \pm 0.005 \text{ eV}$ at $V_D = 5.75 \text{ V}$. The pre-exponential factor $A = 7 \text{ s}^{-1}\text{K}^{-2}$ remains constant at lower fields and it increases slightly to a level of $10 \pm 2 \text{ s}^{-1}\text{K}^{-2}$ at $V_D = 5.75 \text{ V}$. As the temperature decreases below 200 K the emission rate becomes temperature independent. This behavior can be attributed either to the presence of the competing emission mechanisms or to the device self-heating.

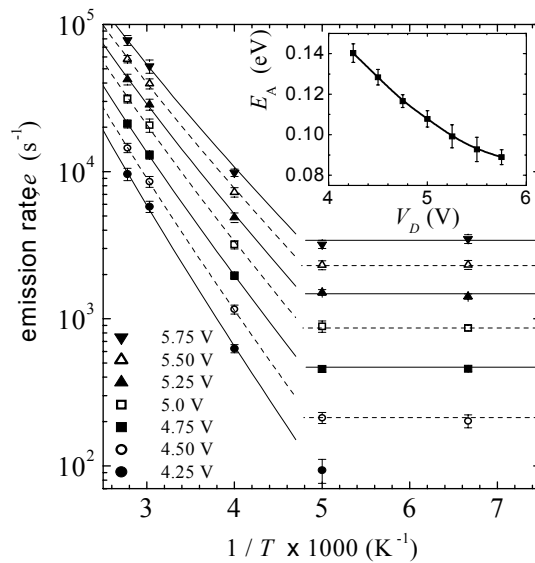


Fig. 2. The emission rate as a function of the inverse temperature measured at different drain voltages. The inset shows the activation energy extracted from the data in the high-temperature regime.

DISCUSSION

Functional dependence of the emission rate on temperature and electric field clearly indicates that the electron emission from the traps follows Poole-Frankel (PF) model of the trap barrier lowering in the presence of electric field [2]. To identify the trapping center, we need to find a universal characteristic, such as the zero-field ionization energy. Knowing the mechanism of the emission enhancement, the zero-field ionization energy can be extrapolated from the activation energy data. Although the apparent activation energy extracted from the temperature dependence of the emission rate is $\sim 0.1\text{--}0.2$ eV, the zero-field ionization energy is significantly higher. The complete model shows that the zero-field ionization energy is $\sim 0.5 \pm 0.1$ eV [2]. The emission rate as a function of the gate-drain voltage at different temperatures is shown in Fig. 3. Solid and dashed lines represent the results of the complete model, which includes the effects of the field-enhanced emission for a charged trap (3D), and a simplified model, which replaces the spherical trap potential with the one-dimensional electrostatic potential. Both models describe the electron emission from the traps with good accuracy.

Identification of the emission mechanism allows unambiguous determination of the binding energy of the trap. In addition, we can deduce other important information such as the trap location and nature. We showed that electron emission from the trap is well described by the PF model, which implies that the trap is described by a long range attractive Coulomb potential. Therefore this trapping center is an ionized donor-like defect. Traps with similar activation energies have been observed in DLTS studies on GaN Schottky diodes [3-5]. The origin of this trap is unknown at this point.

The dependence of the emission rate on the applied field is indicative of the spatial location of the traps. The PF effect implies a direct relationship between the emission rate enhancement and the field acting on the trap. The observed substantial enhancement requires that the strength of the electric field $F = 1 - 3$ MV/cm. This estimate is slightly higher than the field expected in the barrier directly under the gate terminal. Such field can only exist near the drain-side edge of the gate contact, where the field is enhanced by the edge singularity. We note that the estimated value of the field is approaching the breakdown value. However, the extent of the high field region is only few nanometers, which is not enough for an electron to gain sufficient kinetic energy to cause the impact ionization. The gate edge has also the highest probability for electron tunneling from the gate metal into the semiconductor owing to the field singularity. The observed PF effect, therefore, unambiguously identifies the location of the trapping centers: near the drain-edge of the gate contact.

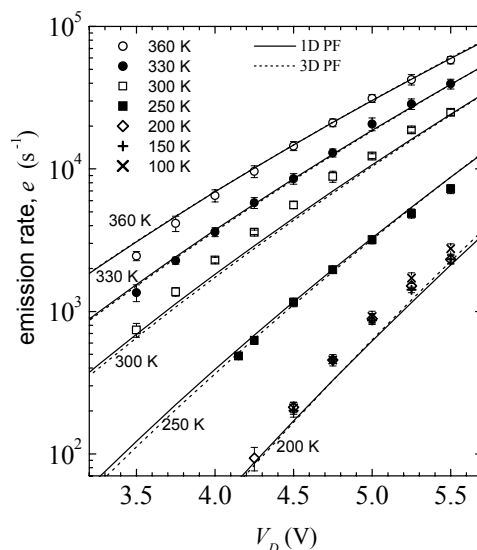


Fig. 3. The emission rate as a function of the gate-drain voltage at different temperatures. Solid and dashed lines represent the fits of the 1D and 3D field-enhanced emission models.

To estimate the density of the occupied traps after the filling pulse, we need to establish a relationship between the change of the channel current and the amount of the trapped charge. The trapped charge Q_T is proportional to the change in the 2DEG density $Q_T = \alpha \Delta n$, where $\alpha = 1$ for the surface traps and $\alpha > 1$ for the traps located under the gate electrode. The 2DEG density in the steady state is $n \cong 10^{13} \text{ cm}^{-2}$ ($V_G = 0 \text{ V}$). In the linear regime, the relative change of the channel current equals to the change of the 2DEG density. Therefore a lower bound for the active trap density can be estimated from the amplitude of the current transient. In our devices we observed trap densities of $Q_T \geq 10^{12} \text{ cm}^{-2}$.

One difficulty with the analysis of trapping behavior in AlGaIn/GaN HEMTs has been the wide variety of phenomena observed by different groups. Timescales from nanoseconds to seconds have been observed in different devices. The vast majority of studies have been performed on samples grown by MOCVD. With this technique it is known that growth conditions can dramatically alter the observed behavior associated with bulk GaN traps. It also appears that device performance depends critically on the treatment of the free surface between the gate and drain.

MBE grown material also exhibit gate lag, however the magnitude of the effect appears to be smaller than that observed for the MOCVD grown structures. In particular, the MBE grown device performance appears to depend less sensitively on surface preparation. This observation is substantiated by the fact that reasonable power densities can be achieved in MBE grown devices without the use surface passivation techniques. One parameter that can dramatically alter the quality of MBE growth is the gallium to nitrogen ratio used in the growth of the GaN buffer region. Growth under nitrogen rich conditions has been associated with rough surface morphologies and increased densities of point defects [6]. The increased rate of formation of point defects may have a serious impact on the observed trapping behavior. Conversely, while growth under Ga rich conditions leads to smooth surface morphologies and higher electron mobilities, any excess Ga accumulated on the surface can alter the electrical nature of threading dislocations, leading to increased reverse-biased gate leakage. In our system, the best films are always grown just below the transition to Ga accumulation on the film surface. This places a very narrow window for optimal growth by MBE. To our knowledge, no systematic study of the influence of Ga surface coverage on gate lag phenomena has been performed. In addition, Si doping of the barrier and capping layers seems to partially mitigate the effect of traps in our devices [7].

CONCLUSIONS

Understanding the mechanisms of gate lag is important for the optimization of the performance and reliability in GaN-based devices. We reviewed the phenomenon in AlGaIn/GaN HEMTs. The major origin of gate lag in these devices is related to electron trapping by the states located on the semiconductor surface and in the transistor barrier. Under the influence of the electric field, electrons tunnel through the gate contact barrier into the semiconductor. The electrons are captured by the traps in the vicinity of the gate edge, causing a partial depletion of the 2DEG in the transistor channel.

Identification of the traps in AlGaIn/GaN HEMTs and their origin is a critical issue. The physical characteristics of the trapping centers as well as their density and location inside the device structure can be deduced using transient current spectroscopy. The technique also allows investigation of the trapping mechanisms. Transient current spectroscopy is particularly valuable because the characterization is performed on actual devices. While the technique has limitations, it provides important information allowing identification of the individual traps, even in the presence of several trapping mechanisms. Substantial help in understanding of the physics of particular traps in GaN can be provided by other characterization techniques, such as optical absorption and luminescence spectroscopy and magnetic resonance spectroscopy. The binding energy of the trap extracted from the transient spectroscopy can be used for correlation to other spectroscopic studies.

Significant research effort is currently directed on trap elimination in GaN-based devices. Careful control of the epilayer growth conditions and surface passivation seem to be the most promising solutions for AlGaIn/GaN HEMTs. Modification of the transistor structure design may be also beneficial. Investigations of gate lag as well as other trapping effects provide insight into the trap elimination problem. With a better understanding of the basic material properties and continuing improvement of its quality, we expect that superior characteristics of GaN will be fully realized.

REFERENCES

1. O. Mitrofanov and M. Manfra, *Appl. Phys. Lett.* 84, 422 (2004).
2. O. Mitrofanov and M. Manfra, *J. Appl. Phys.* 95, 6414 (2004).
3. M.T. Hirsch, J.A. Wolk, W. Walukiewicz, and E.E. Haller, *Appl. Phys. Lett.* 71, 1098 (1997).
4. A. Krtschil, H. Witte, M. Lisker, J. Christen, U. Birkle, S. Einfeldt, and D. Hommel, *J. Appl. Phys.* 84, 2040 (1998).
5. Z.-X. Feng, D.C. Look, P. Visconti, D.-F. Wang, C.-Z. Lu, F. Yun, H.Morkoc, S.S. Park, and K.Y. Lee, *Appl. Phys. Lett.* 78, 2178 (2001).
6. A. Hierro, A. R. Arehart, B. Heying, M. Hansen, U.K. Mishra, S.P. DenBaars, J.S. Speck, and S.A. Ringel, *Appl. Phys. Lett.* 80, 805 (2002).
7. O. Mitrofanov, M. Manfra, and N. Weimann, *Appl. Phys. Lett.* 82, 4361 (2003).